

Energy and Structure of Hard-Sphere Bose Gases in three and two dimensions

F. Mazzanti^a, A. Polls^b and A. Fabrocini^c

^a*Dep. d'Electrònica, Univ. Ramon Llull, Bonanova 8, 08022 Barcelona, Spain*

^b*Dep. ECM, Univ. de Barcelona, Diagonal 645, E-08028 Barcelona, Spain*

^c*Dip. di Fisica, Univ. di Pisa and INFN, Via Buonarroti, 2 I-56100 Pisa, Italy*

The energy and structure of dilute gases of hard spheres in three dimensions is discussed, together with some aspects of the corresponding 2D systems. A variational approach in the framework of the Hypernetted Chain Equations (HNC) is used starting from a Jastrow wavefunction that is optimized to produce the best two-body correlation factor with the appropriate long range. Relevant quantities describing static properties of the system are studied as a function of the gas parameter $x = \rho a^d$ where ρ , a and d are the density, s -wave scattering length of the potential and dimensionality of the space, respectively. The occurrence of a maximum in the radial distribution function and in the momentum distribution is a natural effect of the correlations when x increases. Some aspects of the asymptotic behavior of the functions characterizing the structure of the systems are also investigated.

PACS numbers: 03.75.Hh, 05.30.Jp, 67.40.Db.

1. INTRODUCTION

The study of dilute systems has become a subject of major interest since the achievement of Bose-Einstein condensates in low-density atomic gases confined in harmonic traps. The gas parameter $x = \rho a^d$ where ρ , a and d are the density, s -wave scattering length and space dimensionality (2 or 3 in the cases under study), govern the behavior of the gases in the dilute regime. In the 3D case, an universal dependence of the energy on the scattering length alone has been proved to hold up to values $x \approx 10^{-3}$, while deviations appear at higher x .

In three dimensions, low density expansions can be derived in the framework of standard perturbation theories. Infinite sums of ladder diagrams can

F. Mazzanti, A. Polls, and A. Fabrocini

be carried out and result in the well-known Lee and Yang expansion of the energy per particle ¹

$$E(x) = 4\pi x \left[1 + \frac{128}{15} \sqrt{\frac{x}{\pi}} \right], \quad (1)$$

measured in units of $\hbar^2/2ma^2$.

In two dimensions, logarithmic divergences in the scattering length introduce additional difficulties in the derivation of similar expressions. Still, Schick and Lieb ^{2,3} proved that at low x , the energy per particle of a 2D gas of hard-core bosons satisfies the inequality

$$E(x) \geq \frac{4\pi x}{|\ln x|} \left[1 - \mathcal{O}(\ln x)^{-1/5} \right] \quad (2)$$

in the same units

In this work an analysis of the energy and other properties of 2D and 3D gases of Hard-Sphere bosons is presented ⁴. The starting point is a variational wavefunction of the Jastrow type

$$\Psi_0(\mathbf{r}_1, \mathbf{r}_2, \dots, \mathbf{r}_n) = \prod_{1 \leq i < j \leq N} f(r_{ij}) \quad (3)$$

which is known to accurately account for most of the energy and structure of homogeneous Bose systems at low densities. The minimization of the energy corresponding to the Hard-Spheres potential

$$V(r) = \begin{cases} \infty & r < a \\ 0 & r > a \end{cases} \quad (4)$$

produces a suitable wavefunction that can be used to calculate the energy as well as other, relevant quantities describing the ground state of the system.

2. HNC FORMALISM

The energy per particle of an homogeneous gas of Hard-Sphere bosons described through a Jastrow wavefunction can be expressed in terms of the two-body correlation factor $f(r)$

$$E = -\frac{1}{2}\rho \int d\mathbf{r} g(r) \frac{\hbar^2}{2m} \nabla^2 f(r) \quad (5)$$

and the radial distribution function $g(r)$,

$$g(r_{12}) = \frac{N(N-1)}{\rho^2} \frac{\int d\mathbf{r}_3 d\mathbf{r}_4 \cdots d\mathbf{r}_N |\Psi_0|^2}{\int d\mathbf{r}_1 d\mathbf{r}_2 \cdots d\mathbf{r}_N |\Psi_0|^2}.$$

Energy and Structure of 3D and 2D Bose Gases

One can formally express $f(r)$ as a functional of $g(r)$ and solve the Euler-Lagrange problem $\delta E[g]/\delta g(r) = 0$. This leads to a set of equations which are easily expressed in terms of the static structure function, $S(k) = 1 + \rho \int d\mathbf{r} e^{i\mathbf{k}\cdot\mathbf{r}}(g(r) - 1)$. These can be solved and yield

$$S(k) = \frac{t(k)}{\sqrt{t^2(k) + 2t(k)V_{ph}(k)}} , \quad (6)$$

with $t(k) = \hbar^2 k^2 / 2m$ and $V_{ph}(k)$ the Particle-Hole interaction⁵. In the HNC/0 scheme used throughout this work, elementary diagrams are discarded due to their small contribution at low densities. Then, for a system of Hard Spheres and in r space

$$V_{ph}(r) = \frac{\hbar^2}{m} |\vec{\nabla} \sqrt{g(r)}|^2 + [g(r) - 1] \omega_I(r) , \quad (7)$$

where the k -space induced interaction $\omega_I(k)$ reads

$$\omega_I(k) = -\frac{1}{2} t(k) \frac{[2S(k) + 1][S(k) - 1]}{S^2(k)} . \quad (8)$$

Once with $S(k)$ or $g(r)$ one can get $f(r)$ and compute the momentum distribution $n(k)$

$$n(k) = (2\pi)^d \rho n_0 \delta(\vec{k}) + \int d\vec{r} e^{i\vec{k}\cdot\vec{r}} [\rho_1(r) - \rho n_0] , \quad (9)$$

where n_0 is the condensate fraction and $\rho_1(r)$ is the one-body density matrix

$$\rho_1(r_{11'}) = N \frac{\int d\mathbf{r}_2 \cdots d\mathbf{r}_N \Psi_0(\mathbf{r}_1, \mathbf{r}_2, \dots, \mathbf{r}_N) \Psi_0(\mathbf{r}_{1'}, \mathbf{r}_2, \dots, \mathbf{r}_N)}{\int d\mathbf{r}_1 d\mathbf{r}_2 \cdots d\mathbf{r}_N |\Psi_0|^2} . \quad (10)$$

The momentum distribution is normalized as $1 = \int d\mathbf{k} n(k) / (2\pi)^d \rho$ and its second k -weighted moment provides the kinetic energy per particle.

Notice that for Hard Spheres the potential energy is zero because the product $g(r)V(r)$ vanishes, and therefore the kinetic energy coincides with the total energy of the system.

3. RESULTS

The energy per particle of the gas of Hard Spheres gas is plotted as a function of the gas parameter x in the left panel of Fig. 1, where the Euler-Lagrange solution is compared with Diffusion Monte Carlo results, the low

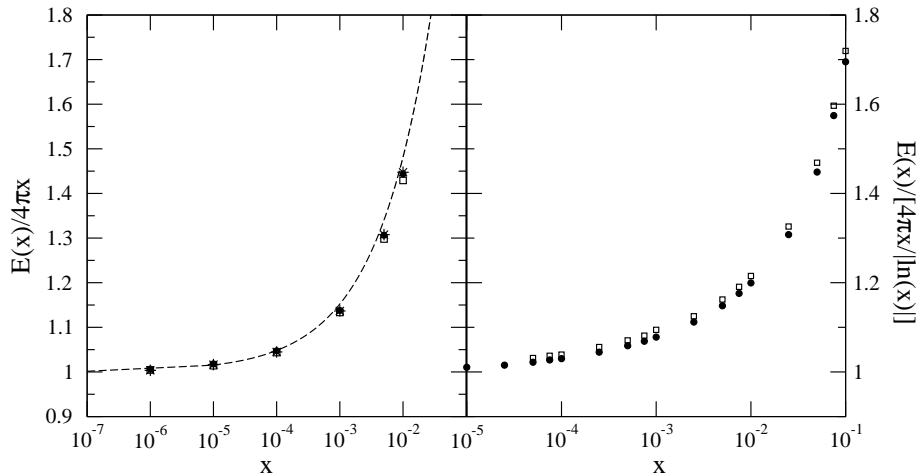


Fig. 1. Energy per particle of the gas of Hard Spheres in 3D and 2D (left and right panels). Solid circles, stars and open squares in the left stand for Euler-Lagrange, HNC/0 and Diffusion Monte Carlo results (the latter taken from Ref. 7. The dashed line represents the low-density expansion of Eq. (1). Solid circles and open squares in the right are Euler-Lagrange and HNC/0 results from the short-ranged $f_{SR}(r)$ of Eq. (12).

density expansion of Eq. (1) and the HNC prediction obtained from a short-ranged two-body correlation function $f_{SR}(r)$. This last function minimizes the lowest order in the cluster expansion of the energy of the homogeneous gas of Hard Spheres with a healing condition at a distance d , taken as a variational parameter ⁶

$$f_{SR}(r) = \begin{cases} 0 & r < a \\ \frac{d}{r} \frac{\sin[K(r-a)]}{\sin[K(d-a)]} & r > a \end{cases}, \quad (11)$$

where K fulfills the equation $\cot[K(d-a)] = (Kd)^{-1}$. As can be seen, differences between the different approximations are not significant up to $x \approx 0.001$. The leading term in the expansion, $E(x) = 4\pi x$, is not enough to correctly account for the energy of the system even at lower values of x , while the inclusion of the second term, which introduces additional dependence on x , improves the agreement. The influence of the optimization on the energy is rather small and the energy is dominated by the short range structure of the potential.

The scaled energy per particle of the gas of Hard Spheres in 2D is shown in right panel of Fig. 1. Euler-Lagrange results are plotted in solid circles and compared with the energy produced by a short range two-body correlation with a healing distance, as in the 3D case. Geometry constrains change the

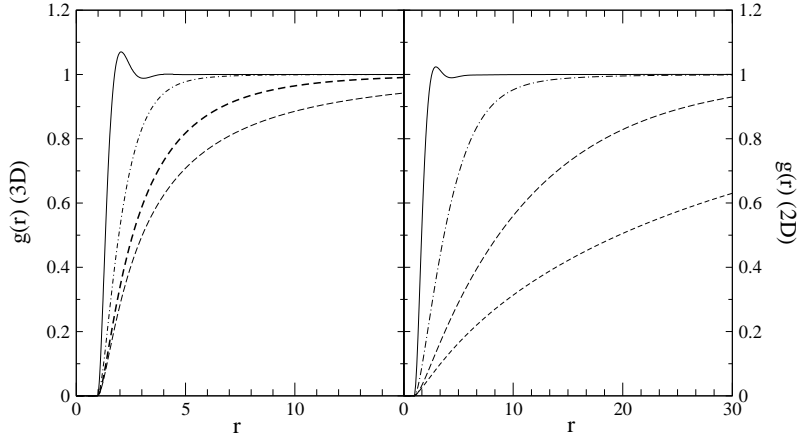


Fig. 2. $g(r)$ for the 3D (left) and 2D (right) gases of Hard Spheres as a function of the gas parameter. Solid line: $x = 10^{-1}$, dot-dashed line: $x = 10^{-2}$, long-dashed line: $x = 10^{-3}$, short-dashed line: $x = 10^{-4}$.

shape of $f_{SR}(r)$ which now reads

$$f(r) = \begin{cases} 0 & r < a \\ \frac{Y_0(\lambda a)J_0(\lambda r) - J_0(\lambda a)Y_0(\lambda r)}{Y_0(\lambda a)J_0(\lambda d) - J_0(\lambda a)Y_0(\lambda d)} & r > a \end{cases} \quad (12)$$

where λ is a Lagrange multiplier satisfying the condition $J_1(\lambda d)Y_0(\lambda a) = J_0(\lambda d)Y_1(\lambda a)$. Energies have been divided by the leading term in Eq. (2) to check convergence towards the limiting case. The agreement of the energy with the corresponding low-density expansion is similar to the 3D case when only the first term $E(x) = 4\pi x$ is considered, while deviations start to be significant at $x \approx 0.001$. In any case, the singular behavior of the energy seems to be entirely taken into account by the logarithmic term, and thus the remaining deviations are expected to be successfully modeled by a smooth function of x that approaches zero when x decreases.

The radial distribution functions of the 3D and 2D gases of Hard Spheres are shown in Fig. 2 for several values of x (left and right panels, respectively). In both cases $g(r)$ develops a peak at $x = 0.1$ that can not be resolved at lower values of x , a clear signature of the effect of correlations. At low x 's, $g(r)$ is a monotonically increasing function of the distance, approaching faster and faster the asymptotic limit $g(r) \rightarrow 1$ with the density. This is more notorious in the 2D case. In fact, this is not surprising if one notices that in 3D and at large distances $g(r) \approx 1 - a/r^4$, while in 2D this behavior changes to $g(r) \approx 1 - b/r^3$, with a, b constants depending on the velocity of sound in the medium.

The final quantity analyzed is the momentum distribution. The product

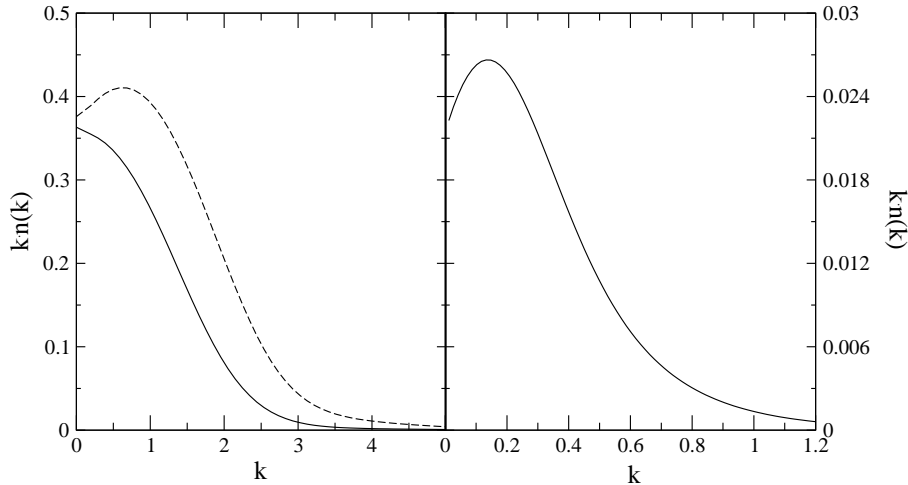


Fig. 3. Momentum distribution of Hard Spheres in 3D and 2D (left and right, respectively). Solid and dashed lines in the left, $x = 0.05$ and $x = 0.08$. Solid line in the right, $x = 0.01$.

$kn(k)$ is shown for the 3D and the 2D cases in Fig. 3. At low x , the momentum distribution is a monotonically decreasing function of k , a behavior already shown by the Bogoliubov approximation at any density. When x increases, $kn(k)$ develops a peak at low k , which can be taken as a genuine effect of long-range correlations. This peak becomes more pronounced and shifts to the right with increasing x . While this maximum is clearly visible already at $x = 0.01$ in 2D, it only shows up at $x > 0.05$ in 3D. As far as the condensate fraction n_0 is concerned, the Bogoliubov estimation in 3D, $n_0^B = 1 - (8/3)\sqrt{x/\pi}$, predicts values that are slightly higher than the ones obtained from the solution of the Euler-Lagrange problem, yielding $n_0^B = 0.850$ against $n_0 = 0.801$ at $x = 0.01$. Larger discrepancies arise at higher values of x . Similar results hold when the EL condensate fraction is compared with Schick's prediction, $n_0^S = 1 + 1/\ln(x)$.

REFERENCES

1. T.D. Lee and C.N. Yang, Phys. Rev. **105**, 1119 (1957); T.D. Lee, K. Huang, and C.N. Yang, *ibid.* **106**, 1135 (1957).
2. M. Schick, Phys. Rev. A **3**, 1067 (1971).
3. E. H. Lieb, and J. Yngvason, J. Stat. Phys. **103**, 509 (2001).
4. F. Mazzanti, A. Polls, and A. Fabrocini, Phys. Rev. A **67**, 063615 (2003).
5. C.C. Chang and C.E. Campbell, Phys. Rev. B **15**, 4238 (1977).
6. V.R. Pandharipande and K.E. Schmidt, Phys. rev. A **15**, 2486 (1977).
7. S. Giorgini, J. Boronat, and J. Casulleras, Phys. Rev. A **60**, 5129 (1999).